Thin Solid Films 612 (2016) 225–230

Contents lists available at ScienceDirect

Thin Solid Films

journal homepage: www.elsevier.com/locate/tsf

The effect of annealing temperature on the optical properties of a ruthenium complex thin film

Kasim Ocakoglu [a,b,*], Salih Okur [c,**], Hasan Aydin [d], Fatih Mehmet Emen [e]

[a] Advanced Technology Research & Application Center, Mersin University, TR-33343, Yenisehir, Mersin, Turkey
[b] Department of Energy Systems Engineering, Faculty of Technology, Mersin University, TR-33480 Mersin, Turkey
[c] Department of Materials Science and Engineering, Faculty of Engineering and Architecture, Izmir Katip Celebi University, Izmir, Turkey
[d] Izmir Institute of Technology, Department of Material Science and Engineering, Gulbahce Campus, 35430, Urla, Izmir, Turkey
[e] Faculty of Arts and Sciences, Department of Chemistry, Mehmet Akif Ersoy University, TR-15030 Burdur, Turkey

ARTICLE INFO

Article history:
Received 11 January 2016
Received in revised form 1 June 2016
Accepted 2 June 2016
Available online 4 June 2016

Keywords:
Thin film
Optical properties
Ruthenium complexes
Annealing

ABSTRACT

The stability of the optical parameters of a ruthenium polypyridyl complex (Ru-PC K314) film under varying annealing temperatures between 278 K and 673 K was investigated. The ruthenium polypyridyl complex thin film was prepared on a quartz substrate by drop casting technique. The transmission of the film was recorded by using Ultraviolet/Visible/Near Infrared spectrophotometer and the optical band gap energy of the as-deposited film was determined around 2.20 eV. The optical parameters such as refractive index, extinction coefficient, and dielectric constant of the film were determined and the annealing effect on these parameters was investigated. The results show that Ru PC K314 film is quite stable up to 595 K, and the rate of the optical band gap energy change was found to be 5.23×10^{-5} eV/K. Furthermore, the thermal analysis studies were carried out in the range 298–673 K. The Differential Thermal Analysis/Thermal Gravimmetry/Differantial Thermal Gravimmetry curves show that the decomposition is incomplete in the temperature range 298–673 K. Ru-PC K314 is thermally stable up to 387 K. The decomposition starts at 387 K with elimination of functional groups such as CO_2, CO molecules and SO_3H group was eliminated between 614 K and 666 K.

1. Introduction

Ruthenium complexes are one of the promising materials for light emitting diodes because of their appropriate photophysical, photochemical, and electrochemical properties [1–5]. Thin films of these complexes also demonstrate significant device performance and optical properties. Especially, ruthenium polypyridyl complexes show significant properties, such as excellent photochemical stability, strong visible absorption, efficient luminescence, and relatively long lived metal to ligand charge transfer (MLCT) excited states [6–9].

A ruthenium polypyridyl complex (Ru-PC K314) was synthesized due to the wide range of application areas, particularly for optoelectronic applications such as solar cells and light emitting diodes [6–9]. In this context, Ru-PC K314 can be considered as a functional material. For instance, this material can also be used for luminescence based sensors [10,11], quartz crystal microbalance based humidity sensors [12], optical pH sensor [13,14] or photovoltaic applications [7–9,15].

The organometallic molecular structure of $[Ru^{II}(L1)_2(L2)]$ is given in Fig. 1, where (L1 = 4,7-diphenyl-1,10-phenanthroline-disulfonic acid disodium salt) and (L2 = 4,4′-dicarboxy-2,2′-bipyridine). There are four sodium sulfonate and two carboxylic acid groups around ruthenium metal. These functional groups bring cationic properties to the material. L1 is chosen not only to increase molar extinction coefficient of the complex, but also to enable the material soluble in water [16]. The compound can also show pH sensitive properties because of the –COOH groups. As a result, it is also soluble in both acidic and basic media [16,17]. L2 is one of the most widely used ligands for ruthenium complexes that employed in Dye Sensitized Solar Cells [7–9,17–20].

Due to the possible applications of the material in solar cells, in this work the Ru-PC K314 complex film was prepared on quartz substrate by drop casting technique, and the stability of the material at high temperatures has been studied. The optical properties of the 480 nm thick film have been investigated in the region of Ultraviolet/Visible/Near Infrared (UV-VIS-NIR). The scope of the present study is to determine the annealing temperature effect on the optical properties (band gap energy, refractive index, dielectric constant) of the film and discussed in detail.

* Correspondence to: K. Ocakoglu, Department of Energy Systems Engineering, Faculty of Technology, Mersin University, TR-33480 Mersin, Turkey.
** Corresponding author.
E-mail addresses: kasim.ocakoglu@mersin.edu.tr (K. Ocakoglu), salih.okur@ikc.edu.tr (S. Okur).

http://dx.doi.org/10.1016/j.tsf.2016.06.004
0040-6090/

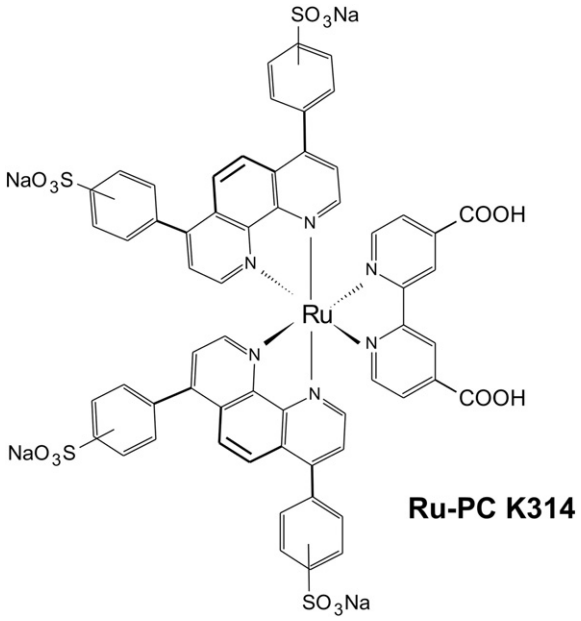

Fig. 1. Chemical structure of ruthenium polypyridyl complex Ru-PC K314, $[Ru(L1)_2(L2)]$.

2. Experimental

[Ru^{II}(bis(4,7-diphenyl-1,10-phenanthroline-disulfonic acid disodium salt) (4,4′-dicarboxy-2,2′-bipyridine)], [Ru-PC K314] (Fig. 1), was synthesized according to the procedure given in the literature [12].

2.1. Preparation and characterization of Ru-PC K314 films

480 nm thick Ru-PC K314 film was prepared according to the following procedure: Organometallic complex (1 mg) was dissolved in 1 mL of toluene. These solutions were deposited onto 2 × 2 cm^2 quartz substrates by drop casting. Organometallic complex (1 mg) was dissolved in 1 ml of toluene, and this freshly prepared solution was deposited by a drop-casting onto 2 × 2 cm^2 quartz substrate. The substrate was then air dried at room temperature. The thicknesses of Ru-PC K314 films were measured by Veeco Dektak profilometer. The optical reflectance (R) and transmittance (T) of the film have been recorded with Shimadzu 2550 UV-Visible spectrophotometer. R and T measurements were repeated several times after annealing the films between 298 K and 673 K for 30 min. The optical parameters were calculated from UV measurements for each annealing temperature. The Differential Thermal Analysis/Thermal Gravimmetry/Differantial Thermal Gravimmetry (DTA/TG/DTG) curves were obtained by using Seiko SII TG/DTA 7200 equipped with DTA and TG units. The thermal analyses were carried out between 298 K and 673 K (heating rate: 10 °C/min). The Pt crucibles were used as sample pan and α-Al_2O_3 was used as the reference material. Measurements were carried out under the dynamic nitrogen atmosphere with a flow rate of 50 mL/min. The sample mass (w_o) was ranged between 5 and 10 mg. To calibrate the temperature, the melting point of indium was used.

3. Results and discussion

3.1. UV/visible optical transmission, reflection and absorption spectroscopy

The spectroscopic properties of the ruthenium complex in solution were investigated via UV-VIS absorption and fluorescence emission spectroscopic studies. Absorption and emission spectra of the complexes were measured in methanol and are shown in Fig. 2. The energy maxima and absorption coefficients are presented in the experimental section. A broad MLCT band, which is well-resolved at 483 nm, is

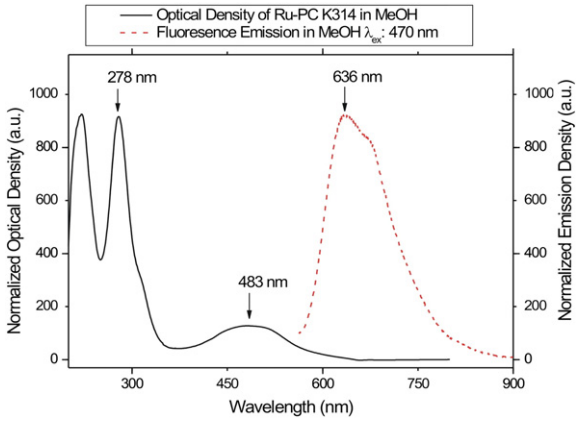

Fig. 2. UV–Vis absorption and emission spectra of Ru-PC K314 measured at ambient temperature under aerobic conditions in MeOH, λ_{ex}: 470 nm.

observed in the absorption spectra. The molar extinction coefficient for this is 13,800 M^{-1} cm^{-1}. These results are very close to the reported MLCT absorptivities of other similar complexes [1,16,20]. The bands at 221 nm and 278 nm and the shoulder observed at around 314 nm can be assigned to the intraligand π-π* transition of the ligands L1 and L2. Emission of the Ru(II) polypyridine complexes usually occur from the lowest-lying MLCT excited state [1,16,20]. When the Ru-PC K314 complex was excited at 470 nm in methanol (MeOH) solution at room temperature, it exhibits a luminescence consisting of a single band with a maximum at 636 nm (Fig. 2).

The optical properties of the film covered with Ru-PC K314 have been investigated using UV-VIS-NIR spectroscopy. Fig. 3(a) and (b) shows a typical transmittance and absorbance of the 480 nm thick film recorded in the wavelength range of 200–700 nm before and

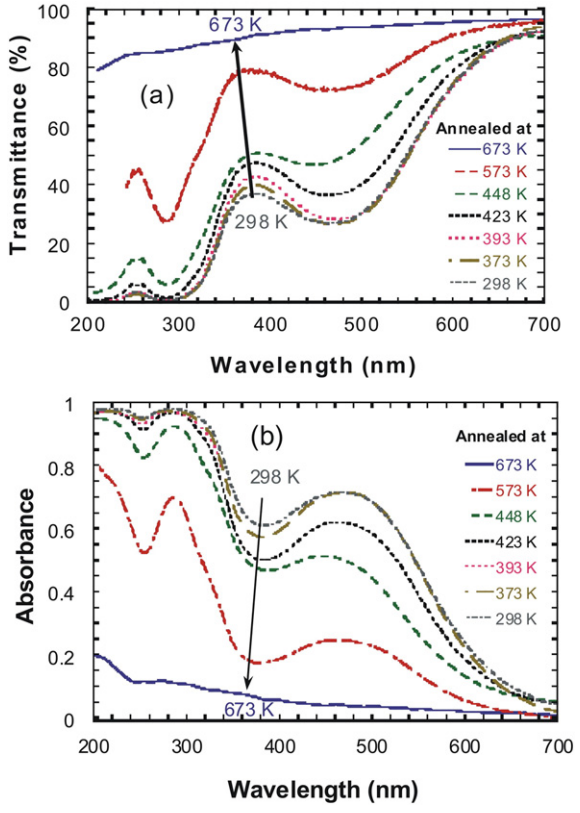

Fig. 3. Transmittance (a) and absorbance (b) of Ru-PC K314 film annealed at different temperatures.

after annealing in the temperature range of 298–673 K. If the annealing temperature is increased up to 573 K, a gradual increase is observed in the transmittance intensities of the Ru-PC K314 film. The peak maxima in the transmission spectrum of the film shift towards lower wavelength with the increasing annealing temperature and all the peaks disappear at 673 K. The absorbance data given in Fig. 3 (b) was calculated from the equation: $A = 1\text{-}(T + R)$ where A denotes absorption, T transmittance and R reflectance. The absorption intensity of the film decreases with increasing annealing temperature. The three major absorption peaks are clearly defined very close to those in MeOH solution at 206 nm, 278 nm and 483 nm. However, since the organic part of the Ru-PC K314 complex decomposes at 673 K the absorbance features disappear.

3.2. The refractive index and optical parameters

The refractive index (n) and absorption coefficient (α) at various wavelengths were calculated by using equations [21];

$$R = \frac{(n-1)^2 + k^2}{(n+1)^2 + k^2}$$
$$T = (1-R)^2 e^{\alpha t}$$

where k is the extinction coefficient ($k = \alpha\lambda/4\pi$), and t is the film thickness. Fig. 4a and b shows that the refractive index n increases from 1.20 to 1.50 with increasing annealing temperature. At 673 K, it becomes approximately constant around 1.50. The extinction coefficient decreases drastically from 0.25 to 0.007 with increasing annealing temperature.

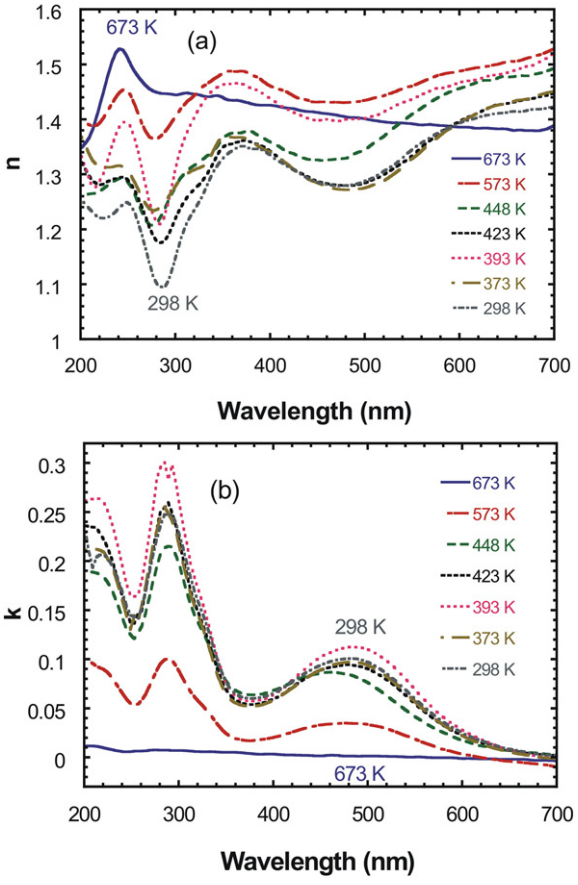

Fig. 4. The variation of the refractive index (a) and extinction coefficient (b) of the thin film at different annealing temperatures.

Table 1
The optical parameter of the Ru-PC K314 film.

Annealing temp. (K)	E_g(eV)	E_0(eV)	E_d(eV)	n_∞	λ_0(nm)	S_0(m^{-2})
298	2.20	4.7	2	1.19	273.2	0.56
373	2.20	4.3	1.7	1.17	292.2	0.44
393	2.17	5.4	3.9	1.16	320.4	0.33
423	2.19	4.4	1.8	1.18	285.1	0.48
448	2.25	5.1	2.7	1.24	244.3	0.88
573	2.20	5.8	4.6	1.34	216.2	1.72
673	3.12	7.8	6.7	1.36	167.8	3.02

The extinction coefficient changes as a function of wavelength for various annealing temperatures except for 673 K. A single broad visible band at 483 nm is assigned to metal-to-ligand charge-transfer origin. Two major extinction coefficient peaks at 221 nm and 280 nm with a shoulder around 314 nm are related to the bands assigned to the intraligand π-π* transition of L1 and L2 ligands as seen in the absorbance plot.

The refractive index dispersion parameters of Ru-PC K314 film can be calculated according to the following expression using single effective oscillator model [22];

$$\frac{n^2_\infty - 1}{n^2 - 1} = 1 - \left(\frac{\lambda_0}{\lambda}\right)^2$$

where n_∞ is the long wavelength refractive index and λ_0 is the average interband oscillator wavelength. The n_∞ and λ_0 values were calculated from the slope of the linear part of the plots of $(1/n^2\text{–}1)$ vs $(h\upsilon)^2$ at various annealing temperatures. The average oscillator strength S_0 values were obtained from $(n^2_\infty\text{-}1)/\lambda_0^2$ [23]. The energy dependence of

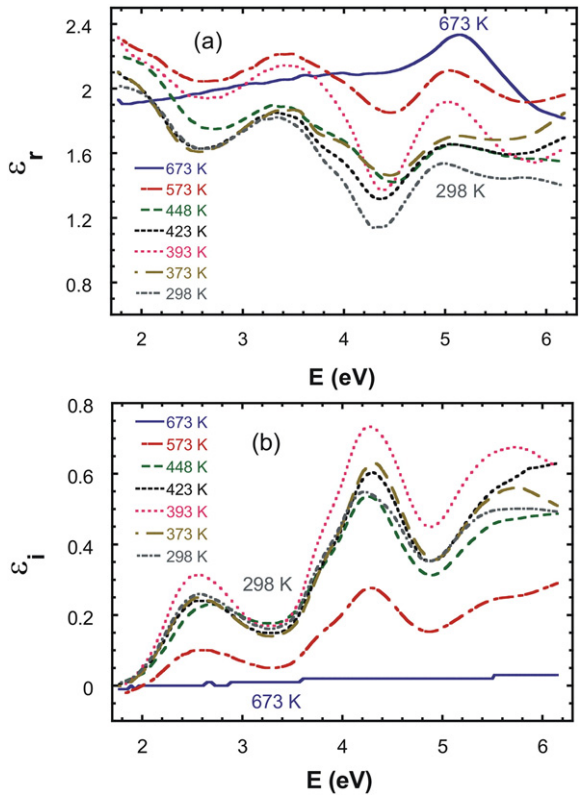

Fig. 5. The real (a) and the imaginary (b) part of the dielectric spectra of the thin film annealed at different temperatures.

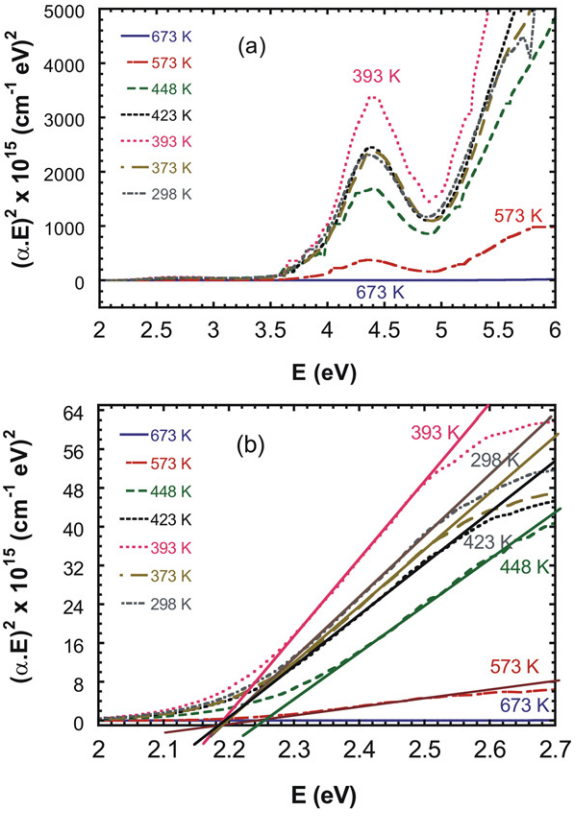

Fig. 6. The plot of $(\alpha h\upsilon)^2$ versus photon energy (a), the high magnification of Fig. 6a between (2.0–2.7 eV) (b) of Ru-PC K314 film annealed at different temperatures.

the refractive index can be expressed according to the following relation [22,24];

$$\frac{1}{n^2}-1=\frac{\left(E_o^2-(h\upsilon)^2\right)}{E_o.E_d}$$

where E_0 is the single oscillator energy and E_d is the dispersion energy. The optical parameters E_0, E_d, n_∞, and χ_0 values are given in Table 1. The single oscillator energy E_0 is obtained around 5.0 eV when annealed below 573 K, and increased to 7.80 eV at 673 K. The long wavelength refractive index n_∞ was obtained around 1.20 when annealed below 573 K and increased to 1.36 eV at 673 K. The average interband oscillator

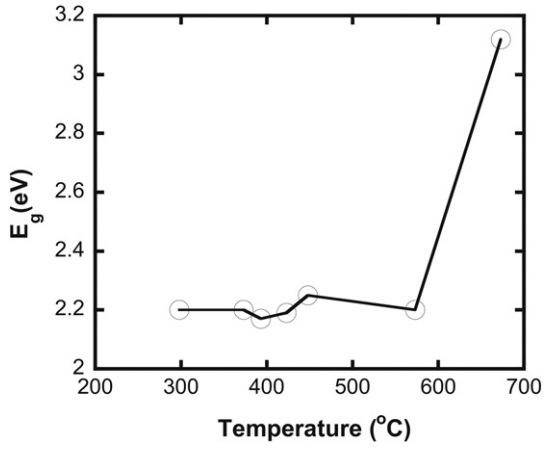

Fig. 7. The variation of the optical band gap with increasing annealing temperature between 278 K and 673 K.

Table 2
Thermoanalytical results of decomposition reaction of Ru-PC K314.

Stage	DTA peak temperature (K)	TG temperature range (K)	Mass loss (%) Exper.	Theor.	Evolved moiety
I	344	298–387	11.32	11.30	$-9H_2O$[a]
II	–	387–614	5.01	5.02	$-CO_2+CO$
III	611 and 636	614–666	6.48	6.42	$-SO_3H$
Residue	–	–	77.19	77.26	$RuC_{58}H_{35}S_3N_6O_{11}Na_4$

[a] In the course of thermogravimetric measurements, moisture content can be easily seen due to the hygroscopic properties of the complex.

wavelength was obtained around 250 nm when annealed below 573 K, and decreased to 167.80 nm at 673 K.

3.3. Dispersion of the optical dielectric constants

The complex dielectric function describes the interaction between the electromagnetic waves and matter. The complex dielectric (ε^*) constant of a material is expressed $\varepsilon^*=\varepsilon_r+\varepsilon_i$ where ε_r is the real and ε_i is the imaginary part of the dielectric constant. Dielectric constant of the Ru-PC K314 film was also calculated using the following relations [21]:

$$\varepsilon_r=n^2-k^2$$
$$\varepsilon_i=2nk$$

The real ε_r and the imaginary part ε_i of the dielectric constant spectra of the Ru-PC K314 film at different annealing temperatures are given in Fig. 5a and b.

The real part ε_r varies in between 1.60 and 2.40, while the imaginary part ε_i increases up to 0.70. Both of the real and imaginary part of the dielectric constant show similar peaks as seen in refractive index n and extinction coefficient k for the annealing temperature between 298 K and 573 K except for 673 K, since Ru-PC K314 decomposes partially at this temperature.

3.4. The determination of optical band gap energy

The optical band gap energy E_g of a film can be evaluated from its absorption spectrum depending on whether it has direct or indirect transitions. For the band gap energy calculation of the film, the following relation is used [25]:

$$\alpha h\nu=A(h\nu-E_g)^m$$

where A is a constant associated with the extent of the band tails. The exponent m is 1/2 and 2 for allowed and forbidden direct transitions,

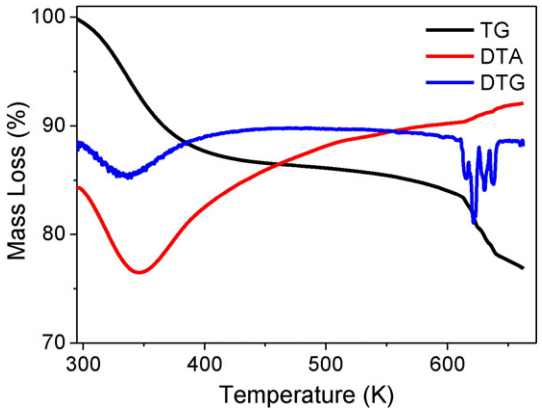

Fig. 8. DTA/TG/DTG curves of Ru-PC K314.

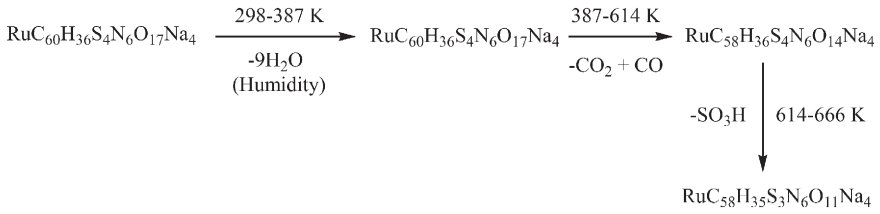

Scheme 1. The suggested pre-decomposition mechanism Ru-PC K314.

respectively. The optical band gap energy of the Ru-PC K314 films between The Highest Occupied Molecular Orbital (HOMO) and The Lowest Unoccupied Molecular Orbital (LUMO) bands can be estimated by assuming direct transitions [26]. The $(\alpha h\nu)^2$ versus energy E(eV) plots of Ru-PC K314 film for the annealing temperatures between 278 K and 673 K are shown in Fig. 6. The E_g of the film can be estimated from the intercept of a line fit to the linear part of $(\alpha h\nu)^2$ versus energy E(eV) plots. The optical band gap energy values of Ru-PC K314 film for various annealing temperatures estimated from Fig. 6, and are listed in Table 1.

Two peaks in the absorption band edges around 2.2 eV and 3.7 eV are related to the intraligand π-π* transition of L1 and L2 ligands resulting emission from the lowest-lying ^{3}MLCT excited state in Ru(II) polypyridine complexes.

Table 1 shows the optical parameters of Ru-PC K314 thin film at various temperatures. The variation of the optical band gap with increasing annealing temperature between 278 K and 673 K are shown in Fig. 7. The optical energy gap E_g of Ru-PC K314 film is quite stable with increasing annealing temperatures between 278 K and 573 K. However, it increases dramatically to 3.12 eV due to the decomposition of the organic part of Ru-PC K314 complex. The optical band gap of semiconductors changes linearly with change in temperature. Fig. 7 shows the change of fundamental energy gap with increasing annealing temperature. The rate of the band gap energy changes for the annealing temperatures below 573 K is obtained as 5.23×10^{-5} eV/K. This change is attributed to the increase in the interatomic distances arising from electron-lattice interaction [27]. The absorption feature starting around 2.20 eV corresponds to the so called *onset energy gap* (Q-band) while the absorption starting around 3.70 eV corresponds to the *fundamental energy gap* (B-band or Soret band) [28,29]. The onset energy gap disappears when the Ru-PC K314 film is annealed at $T > 595$ K due the degradation of organic part of the complex, and remaining ruthenium residue on the quartz substrate.

3.5. Thermal stability of Ru-PC K314

The thermal stability of Ru-PC K314 was studied by using thermal analysis techniques from 298 K up to 673 K under nitrogen atmosphere (50 mL/min.). The temperature range of the decomposition, DTA peak positions and mass losses of the decomposition reactions are given in Table 2.

DTA/TG/DTG curves of Ru-PC K314 are shown in Fig. 8. TGA curves are similar to our previous reports [30,31]. The pre-decomposition of Ru-PC K314 was carried out in three stages at selected temperature range (298–673 K). The first decomposition stage was shown in the temperature range of 298–387 K in TG and DTG curves. The experimental mass loss was determined about 11.32% (calc. 11.30%). The elimination of 9 mol of H_2O from coordination sphere of Ru-PC K314 was occurred due to hygroscopic properties of Ru-PC K314. The second decomposition stage was observed between 387 K and 614 K with the experimental mass loss of 5.01% (calc. 5.02%). 1 mol of CO and 1 mol of CO_2 were eliminated from Ru-PC K314. The remaining intermediate product was estimated to be $RuC_{58}H_{36}S_4N_6O_{14}Na_4$. The third decomposition stage occurs between 614 K and 666 K with elimination of 1 mol SO_3H. The experimental and calculated mass losses were 6.40% and 6.42%, respectively. The residue product of this stage was estimated as $RuC_{58}H_{35}S_3N_6O_{11}Na_4$.

It can be seen three endothermic peaks were obtained in DTA curve of Ru-PC K314 in Fig. 8. The minima of the DTA peaks are 344 K, 611 K and 636 K, respectively. The first endothermic peak corresponds to elimination of H_2O and the others correspond to pre-decomposition of Ru-PC K314. In addition, DTG peaks are observed at 337 K, 615 K, 621 K, 631 K and 637 K which correspond to pre-decomposition of Ru-PC K314, too.

According to DTA/TG/DTG data, the decomposition mechanism of Ru-PC K314 can be given as in Scheme 1.

4. Conclusion

The stability of the optical parameters of a ruthenium polypyridyl complex (Ru-PC K314) film under varying annealing temperatures between 278 K and 673 K was investigated using UV-VIS-NIR spectroscopy. The optical gap energy of Ru-PC K314 film was determined as 2.20 eV. The results show that Ru PC K314 film is quite stable up to 573 K and the rate of change of optical energy gap was obtained as 5.23×10^{-5} eV/K. The optical band gap increases dramatically to 3.12 eV due to the degradation of organic part of Ru-PC K314. The thermal analysis results show that Ru-PC K314 is stable up to 387 K. After this temperature, the decomposition starts with elimination of functional groups such as CO_2, CO and SO_3H molecules. The decomposition is incomplete in the temperature range 298–673 K. These results show that Ru-PC K314 films are quite stable for the solar cell applications for the working temperatures up to 595 K.

Acknowledgements

This research was partially supported by DPT (State Planning Organization of Turkey) under project number DPT2003K120390 and by The Scientific and Technological Research Council of Turkey, TUBITAK under Grant No. TBAG-109T240.

References

[1] K. Ocakoglu, C. Zafer, B. Cetinkaya, S. Icli, Synthesis, characterization and spectroscopic studies of two new heteroleptic Ru(II) polypyridyl complexes, Dyes Pigments 75 (2) (2007) 385.
[2] H. Rudmann, S. Shimada, M.F. Rubner, Solid-state light-emitting devices based on the tris-chelated ruthenium(II) complex. 4. High-efficiency light-emitting devices based on derivatives of the tris(2,2′-bipyridyl) ruthenium(II) complex, J. Am. Chem. Soc. 124 (17) (2002) 4918.
[3] E. Tekin, E. Holder, V. Marin, B.J. de Gans, Ink-jet printing of luminescent ruthenium- and iridium-containing polymers for applications in light-emitting devices, U.S. Schubert, Macromol. Rapid Commun. 26 (4) (2005) 293.
[4] F. Barigelletti, L. Decola, V. Balzani, R. Hage, J.G. Haasnoot, J. Reedijk, J.G. Vos, Photophysical, photochemical, and electrochemical properties of mononuclear and dinuclear ruthenium(ii) complexes containing 2,2′-bipyridine and the 3,5-bis(pyridin-2-yl)-1,2,4-triazolate ion, Inorg. Chem. 28 (24) (1989) 4344.
[5] R.T.F. Jukes, B. Bozic, F. Hartl, P. Belser, L. De Cola, Synthesis, photophysical, photochemical, and redox properties of nitrospiropyrans substituted with Ru or Os tris(bipyridine) complexes, Inorg. Chem. 45 (20) (2006) 8326.
[6] M. Buda, G. Kalyuzhny, A.J. Bard, Thin-film solid-state electroluminescent devices based on tris(2,2′-bipyridine)ruthenium(II) complexes, J. Am. Chem. Soc. 124 (21) (2002) 6090.
[7] K. Ocakoglu, F. Yakuphanoglu, J.R. Durrant, S. Icli, Thin-film solid-state electroluminescent devices based on tris(2,2′-bipyridine)ruthenium(II) complexes, Sol. Energy Mater. Sol. Cells 92 (9) (2008) 1047.

[8] M. Grätzel, Conversion of sunlight to electric power by nanocrystalline dye-sensitized solar cells, J. Photochem. Photobiol. A 164 (3) (2004) 3.
[9] S. Icli, C. Zafer, K. Ocakoglu, Y. Teoman, Patent Application File, WO2009078823 (A1) 2009.
[10] S.M. Ji, W.H. Wu, W.T. Wu, P. Song, K.L. Han, Z.G. Wang, S.S. Liu, H.M. Guo, J.Z. Zhao, Tuning the luminescence lifetimes of ruthenium(II) polypyridine complexes and its application in luminescent oxygen sensing, J. Mater. Chem. 20 (2010) 1953–1963.
[11] O. McGaughey, J.V. Ros-Lis, A. Guckian, A.K. McEvoy, C. McDonagh, B.D. MacCraith, Development of a fluorescence lifetime-based sol-gel humidity sensor, Anal. Chim. Acta 570 (1) (2006) 15–20.
[12] K. Ocakoglu, S. Okur, Humidity sensing properties of novel ruthenium polypyridyl complex, Sensors Actuators B Chem. 151 (1) (2010) 223.
[13] R. Grigg, W.D. Norbert, Luminescent pH sensors based on di(2,2′-bipyridyl) (5,5′-diaminomethyl-2,2′-bipyridyl)ruthenium(II) complexes, Chem. Commun. (18) (1992) 1300.
[14] J.M. Price, W.Y. Xu, J.N. Demas, B.A. DeGraff, Polymer-supported pH sensors based on hydrophobically bound luminescent ruthenium(II) complexes, Anal. Chem. 70 (2) (1998) 265.
[15] P. Wang, S.M. Zakeeruddin, J.E. Moser, M.K. Nazeeruddin, T. Sekiguchi, M. Grätzel, A stable quasi-solid-state dye-sensitized solar cell with an amphiphilic ruthenium sensitizer and polymer gel electrolyte, Nat. Mater. 2 (6) (2003) 402.
[16] K. Ocakoglu, Y. Yildirim, F.Y. Lambrecht, J. Ocal, S. Icli, Biological investigation of I-131-labeled new water soluble Ru(II) polypyridyl complex, Appl. Radiat. Isot. 66 (2) (2008) 115.
[17] M.K. Nazeeruddin, M. Grätzel, Separation of linkage isomers of trithiocyanato (4,4′,4″-tricarboxy-2,2′,6,2″-terpyridine)ruthenium(II) by pH-titration method and their application in nanocrystalline TiO_2-based solar cells, J. Photochem. Photobiol. A Chem. 145 (1–2) (2001) 79.
[18] M.K. Nazeeruddin, S.M. Zakeeruddin, J.J. Lagref, P. Liska, P. Comte, C. Barolo, G. Viscardi, K. Schenk, M. Graetzel, M. Coordin, Synthesis of novel ruthenium sensitizers and their application in dye-sensitized solar cell, Chem. Rev. 248 (13–14) (2004) 1317.
[19] C. Sahin, C. Tozlu, K. Ocakoglu, C. Zafer, C. Varlikli, S. Icli, Synthesis of an amphiphilic ruthenium complex with swallow-tail bipyridyl ligand and its application in nc-DSC, Inorg. Chim. Acta 361 (3) (2008) 671.
[20] M.K. Nazeeruddin, R. Humphry-Baker, P. Liska, M. Grätzel, Investigation of sensitizer adsorption and the influence of protons on current and voltage of a dye-sensitized nanocrystalline TiO_2 solar cell, J. Phys. Chem. B 107 (34) (2003) 8981.
[21] N. Kojima, Y. Sugiura, M. Yamaguchi, Optical properties of C60/a-C superlattice structures for solar cell applications, Sol. Energy Mater. Sol. Cells 90 (18–19) (2006) 3394.
[22] S.H. Wemple, M. Di Domenico, Behavior of the electronic dielectric constant in covalent and ionic materials, Phys. Rev. B 3 (4–15) (1971) 1338.
[23] P.A. Lee, G. Said, R. Davis, T.H. Lim, On the optical properties of some layer compounds, J. Phys. Chem. Solids 30 (19) (1969) 2719.
[24] S.H. Wemple, Refractive-index behavior of amorphous semiconductors and glasses, Phys. Rev. B 7 (8–15) (1972) 3767.
[25] E.A. Davis, N.F. Mott, Conduction in non-crystalline systems V. Conductivity, optical absorption and photoconductivity in amorphous semiconductors, Phil. Mag. 22 (179) (1970) 903.
[26] H.Y. Zhang, C.Y. Wu, L.Z. Liang, Y.M. Chen, Y.Y. He, Y.J. Zhu, N. Ke, J.B. Xu, S.P. Wong, A.X. Wei, S.Q. Peng, Structural, morphological and optical properties of C-60 cluster thin films produced by thermal evaporation under argon gas, J. Phys. Condens. Matter 13 (13) (2001) 2883.
[27] Y. Atalay, A. Basoglu, D. Avci, M. Arslan, T. Ozturk, E. Ertas, Determination and analysis of the dispersive optical constants of the 5,5′,6,6′-tetraphenyl-2,2′-bi([1,3]dithiolo[4,5-*b*][1,4]dithiinylidene)–DDQ complex thin film, Physica B 403 (12) (2008) 1983.
[28] M.M. El-Nahass, F.S. Bahabri, R. Al-Harbi, Optical properties of copper phthalocyanine (CuPc) thin films, Egypt, J. Sol. 24 (1) (2001) 11.
[29] M. Wojdyla, B. Derkowska, W. Bala, A. Bratkowski, A. Korcala, Investigation of optical transition energy in copper phthalocyanine by transmission, reflection and photoreflectance spectroscopy, Opt. Mater. 28 (8) (2005) 1000–1005.
[30] K. Ocakoglu, F.M. Emen, Thermal analysis of *cis*-(dithiocyanato)(1,10-phenanthroline-5,6-dione)(4,40-dicarboxy-2,20-bipyridyl)ruthenium(II) photosensitizer, J. Therm. Anal. Calorim. 104 (2011) 1017–1022.
[31] K. Ocakoglu, F.M. Emen, N. Kulcu, An investigation of decomposition stages of a ruthenium, polypridyl complex by non-isothermal methods, J. Therm. Anal. Calorim. 110 (2012) 799–805.